ISSN 1846-6168 (Print), ISSN 1848-5588 (Online)
https://doi.org/10.31803/tg-20230427105045

Original scientific paper
Received: 2023-04-27, Accepted: 2023-05-10

PID Control of Hybrid DC-DC Converter System in Complex Load with Double Reference Time

Erol Can*, Murat Gülnahar

Abstract: DC-DC converters are circuits that are widely used in energy distribution systems, in industry and technology applications, as well as in household appliances such as computers and televisions, and in uninterruptible power supplies used to feed all these systems. For the design and optimization of DC-DC converter circuits, it is important to create and analyze mathematical models according to the load it is connected to. Simple load structures and circuit structures have been examined and control units have been designed in studies carried out to date. In this study, while the DC-DC converter with a more complex load structure is discussed, mathematical analysis and PID control of DC-DC converters with Buck-Boost feature are performed with the same modulation index in different time periods. In the results obtained, it is shown how to create the mathematical models of a system that provides DC-DC energy conversion with a complex load structure and how to formulate the PID control in a system with this complex load structure.

Keywords: analyze mathematical models; complex load structure; DC-DC converters; uninterruptible power supplies

1 INTRODUCTION

DC-DC converters are power circuits that provide a variable dc voltage to the load they feed, different from the source voltage level applied to them [1-3]. These power circuits can perform balancing tasks between variable input power supplies and the load as in[4-7]. The performance of switched power circuits enables power conversion between the ac source and batteries in devices with low-power household appliances such as computers while minimizing the battery structure of the system in the circuits [8]. Since solar photovoltaics are renewable energy sources that are easy to install, they can be preferred for electrical devices as a suitable method for battery charging [9]. DC-DC converters are needed to connect solar cells to electrical devices and to provide energy balance [10, 11]. In order to increase efficiency and stability in energy systems, the design, analysis, and control of power circuits that provide transformation in the system are of great importance [12, 13]. In order to optimize and control the DC-DC converter structures, the mathematical structure of the system should be analyzed and created [14, 15]. Although there are DC-DC converter studies for many important applications, DC-DC converters with complex loads in the studies presented so far are limited to presenting the analysis and mathematical structure of the structure [15, 16]. Although this converter structure is examined in open loop control, traditional converter time-dependent mathematical models and losses in MOSFET structure are examined for simple load structure [17]; Closed-loop PID controlled transfer functions in the S domain have not been investigated in the complex load structure. Therefore, this article examines the PID control of a multi-reference DC-DC converter structure with a complex load structure. Mathematical models of circuit structure with complex load structures such as R, RL, RLC, and parallel series R//RL are derived. The mathematical functions of the PID control are built into the extracted mathematical models of the circuit. PI and PID applications of circuits are made in Matlab Simulink, and converters with complex loads are optimized. In the results obtained, while the mathematical circuit model analysis of the converter with complex load structure was obtained, satisfactory results were obtained in terms of both the current and voltage level on the used loads and the residence times.

2 HYBRID BUCK BOOST CONVERTER MATHEMATICAL MODELS AT DIFFERENT COMPLEX LOADS AND SIMULATION STUDIES

In Fig. 1a, the circuit structure of the hybrid DC-DC converter with R load is given. In Fig. 1b, the block diagram showing the control of the R-loaded circuit is given.

There are two transfer functions F_{S1} and F_{S2} for the two time slots that give the working characteristics of the proposed circuit. I_{L1} is the current of coil L_1 while I_{L2} is the current of coil L_2. V_o is output voltage. F_{S1} and F_{S2} are transfer functions that represent circuit models during periods of different reference values. The circuits represented by these functions are different converter structures. F_{S1} can be arranged as in the equations below.

$$V_{dc} = V_i = L_{L1}\left[L_1 s + \left(\frac{1}{R} + Cs\right)^{-1}\right] \tag{1}$$

$$V_{dc} = V_i = L_{L1}\left[L_1 s + \left(\frac{1+RCs}{R}\right)^{-1}\right] \tag{2}$$

$$V_{dc} = V_i = L_{L1}\left[\frac{R + L_1 s + L_1 sRCs}{1+RCs}\right] \tag{3}$$

$$V_i = L_{L1}\left[\frac{R + L_1 s + RCL_1 s^2}{1+RCs}\right] \tag{4}$$

$$V_o = L_{L1}\left[\frac{R}{1+RCs}\right] \tag{5}$$

$$F_{S1} = \frac{V_o}{V_i} = \frac{L_{L1}\left[\frac{R}{1+RCs}\right]}{L_{L1}\left[\frac{R + L_1 s + RCL_1 s^2}{1+RCs}\right]} \tag{6}$$

$$F_{S1} = \left[\frac{R}{1+RCs}\right]\left[\frac{1+RCs}{R+L_1 s+RCL_1 s^2}\right] \quad (7)$$

$$F_{S1} = \left[\frac{R}{R+L_1 s+RCL_1 s^2}\right] \quad (8)$$

For F_{S2}, system transfer function calculated as below:

$$V_{dc} = V_i = L_{L2} L_2 s \quad (9)$$

$$V_o = L_{L2}\left[\frac{R}{1+RCs}\right] \quad (10)$$

$$F_{S2} = \frac{V_o}{V_i} = \frac{L_{L2}\left[\frac{R}{1+RCs}\right]}{L_{L2} L_2 s} \quad (11)$$

$$F_{S2} = \left[\frac{R}{1+RCs}\cdot\frac{1}{L_2 s}\right] \quad (12)$$

$$F_{S2} = \left[\frac{R}{L_2 s+RCL_2 s^2}\right] \quad (13)$$

When the total t time is considered as the working time of the two modes, the working rates to be determined by the time durations of the two functions are as given in the matrix form below.

$$\begin{bmatrix} F_{S1} \\ F_{S2} \end{bmatrix} = \begin{bmatrix} \frac{R}{R+L_1 s+RCL_1 s^2} & 0 \\ 0 & \frac{R}{L_2 s+RCL_2 s^2} \end{bmatrix} \begin{bmatrix} \frac{t_1}{(t_1+t_2)} \\ \frac{t_2}{(t_1+t_2)} \end{bmatrix} \quad (14)$$

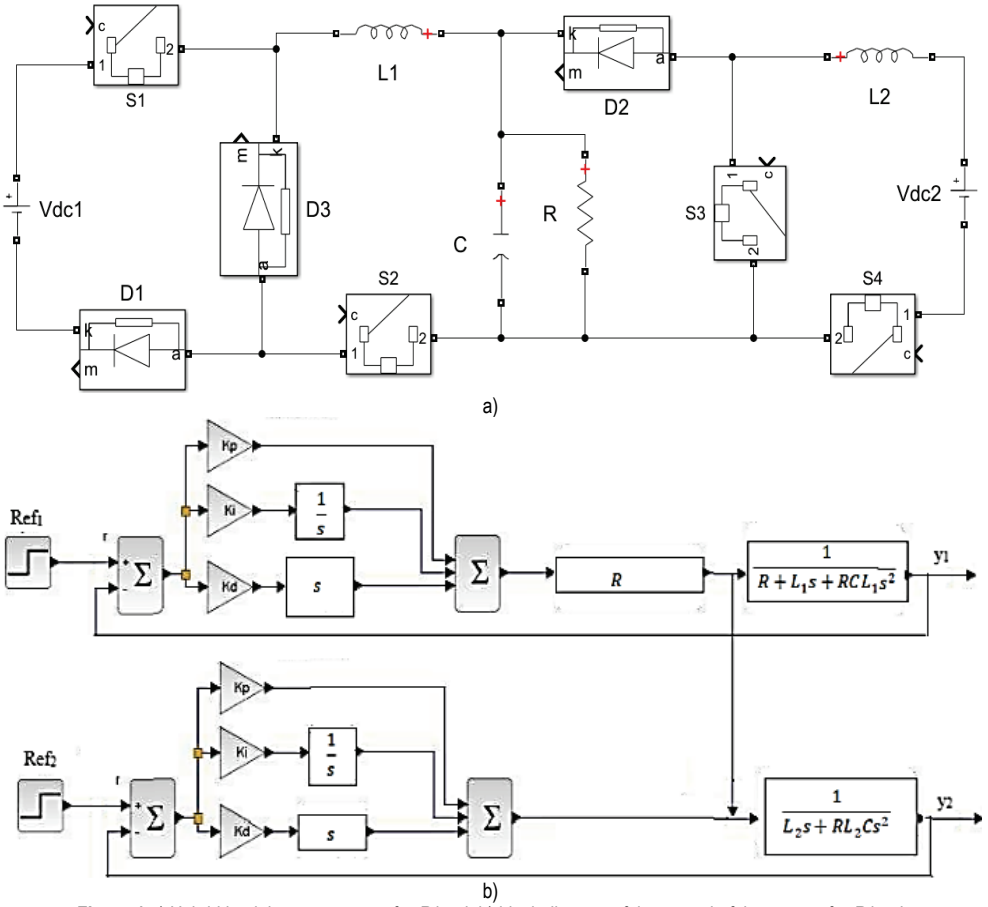

Figure 1 a) Hybrid buck boost converter for *R* load, b) block diagram of the control of the system for *R* load

Arrangements are made to provide PID control of the system to the multi-time transfer functions of the power circuit. PID (Proportional Integral Derivative) is one of the most used control methods today. P represents proportional controller; I represent integral controller and D represents derivative controller. K_p is gain for Proportional, K_i is gain for Integral, K_d is gain for Derivative. To create a system control where the error is close to zero, the output signal of the controlled system is fed back and compared with the specified reference signal. A driver signal obtained based on the comparisons between the input and output signals is calculated by the PID controller and applied to the system to reduce the error to zero. In this way, the error value is tried to be brought to zero. However, while resetting the error, attention should be paid to the overshoot and settling time values of the system. There are many different methods to find the coefficients of the PID controller. In slow and lagging systems such as temperature control, Ziegler-Nichols

should be preferred because it is easy to use and also gives a good starting point to reach suitable PID coefficients [16, 18]. PID can be applied to the mathematical model of the generated power circuit for R load as shown in the equation matrix below.

$$\begin{bmatrix} F_{S1} \\ F_{S2} \end{bmatrix} = \begin{bmatrix} \dfrac{K_d s^2 + (K_p + R)s + K_i}{(RCL_2)s^3 + (L_2 + K_d)s^2 + (K_p)s + K_i} & 0 \\ 0 & \dfrac{K_d s^2 + (K_p + R)s + K_i}{(RCL_1)s^3 + (L_1 + K_d)s^2 + (K_p + \mathrm{R})s + K_i} \end{bmatrix} \begin{bmatrix} \dfrac{t_1}{(t_1 + t_2)} \\ \dfrac{t_2}{(t_1 + t_2)} \end{bmatrix} \quad (15)$$

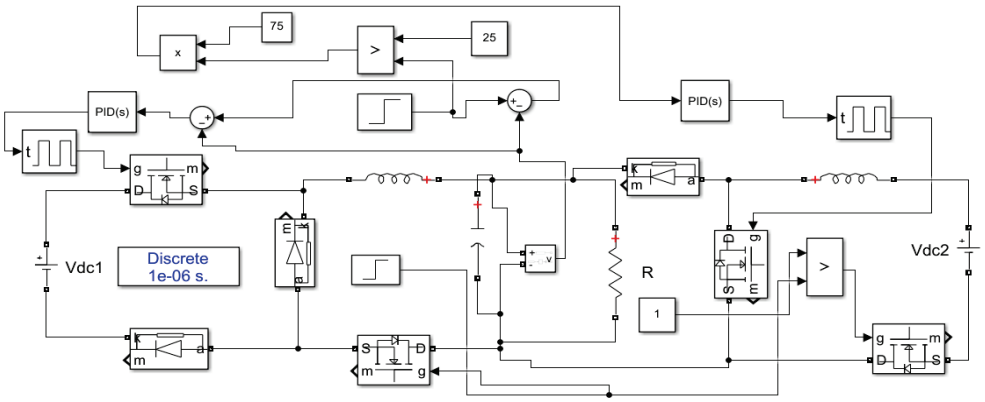

Figure 2 The MATLAB Simulink model of the created power circuit for R load

The MATLAB Simulink model of the created power circuit for the R load is given in Fig. 2. There are 2 DC voltage sources of 50 V in the circuit. While I_{L1} and I_{L2} are 0.1 mH, C is 3 mF. A 3-ohm resistive load is used as a load. Square PWM is used to control the semiconductor power switches in the system. Although the operating ratio (D) for these PWMs is determined as 50%, the PID closed loop control differentiates the operating ratios by comparing the reference values with the output values. When the system is controlled with P = 5 and I = 1 values and PI controls, the current and voltage on the load are formed as given in Fig. 3a. The settling time of current and voltage takes place in 0.04 s. For Boost mode, while 101 V voltage is applied to the load, the current passing through the load is 33.6 A. The electrical energy power conversion obtained for RL load in boost mode is 3393.6 W. For Buck mode, while a voltage of 33 V can be applied to the load on the load, a current of 11 A flows over the load. The electrical energy power conversion obtained for RL load in boost mode is 363 W. When the system is controlled by PID controls with P = 5, I = 1 and D = 0.2 values, the current and voltage on the load are formed as given in Fig. 3b. The settling time of current and voltage takes place in 0.01 s. This provides a 75% improvement in the settling time. For Boost mode, while 101 V voltage is applied to the load, the current passing through the load is 33.6 A. For Buck mode, while a voltage of 33 V can be applied to on the load, a current of 11 A passes through the load.

The circuit model of the converter circuit for R and L load is given in Fig. 4. The mathematical models of the transfer function of the circuit according to the series connected RL load can be arranged as follows.

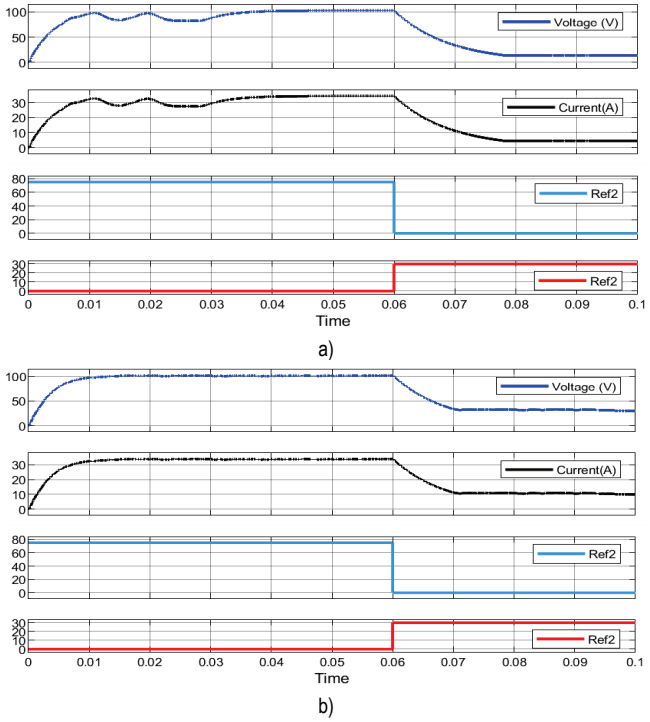

Figure 3 a) PI control for R load, b) PID control for R load

$$V_{dc} = V_i = L_{L1}\left[L_1 s + \left(\frac{1}{R + Ls} + Cs\right)^{-1}\right] \quad (16)$$

$$V_{dc} = V_i = L_{L1}\left[L_1 s + \left(\frac{1 + RCsLs + RCs}{R + Ls}\right)^{-1}\right] \quad (17)$$

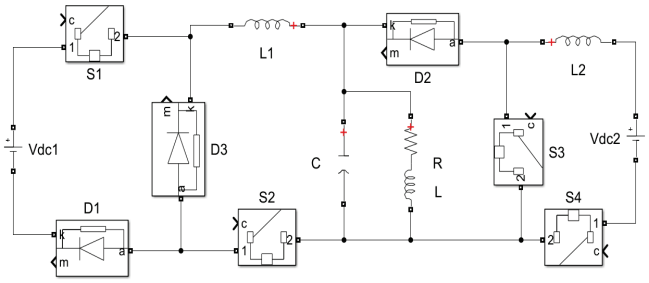

Figure 4 Power circuit model for RL load

$$V_{\mathrm{i}} = L_{\mathrm{L1}}\left[L_1 s + \left(\frac{R+Ls}{RCLs^2+RCs+1}\right)\right] \tag{18}$$

$$V_{\mathrm{i}} = L_{\mathrm{L1}}\left[\frac{RCLL_1s^3+RCL_1s^2+(L_1+L)s+R}{RCLs^2+RCs+1}\right] \tag{19}$$

$$V_{\mathrm{o}} = I_{\mathrm{L1}}\left(\frac{R+Ls}{RCLs^2+RCs+1}\right) \tag{20}$$

$$F_{\mathrm{S1}} = \frac{I_{\mathrm{L1}}\left(\frac{R+Ls}{RCLs^2+RCs+1}\right)}{I_{\mathrm{L1}}\left(\frac{RCLL_1s^3+RCL_1s^2+(L_1+L)s+R}{RCLs^2+RCs+1}\right)} \tag{21}$$

$$F_{\mathrm{S1}} = \left(\frac{R+Ls}{RCLs^2+RCs+1}\right)\left(\frac{RCLs^2+RCs+1}{RCLL_1s^3+RCL_1s^2+(L_1+L)s+R}\right) \tag{22}$$

$$F_{\mathrm{S1}} = \left(\frac{R+Ls}{RCLL_1s^3+RCL_1s^2+(L_1+L)s+R}\right) \tag{23}$$

For F_{S2}, system transfer function calculated as below:

$$V_{\mathrm{dc}} = V_{\mathrm{i}} = L_{\mathrm{L2}}L_2 s \tag{24}$$

$$V_{\mathrm{o}} = I_{\mathrm{L2}}\left(\frac{R+Ls}{RCLs^2+RCs+1}\right) \tag{25}$$

$$F_{\mathrm{S2}} = \frac{V_{\mathrm{o}}}{V_{\mathrm{i}}}\frac{I_{\mathrm{L2}}\left(\frac{R+Ls}{RCLs^2+RCs+1}\right)}{I_{\mathrm{L2}}L_2 s} \tag{26}$$

$$F_{\mathrm{S2}} = \left[\frac{R+Ls}{RCLs^2+RCs+1}\cdot\frac{1}{L_2 s}\right] \tag{27}$$

$$F_{\mathrm{S2}} = \left[\frac{R+Ls}{RCLL_2s^3+LL_2s^2+L_2s}\right] \tag{28}$$

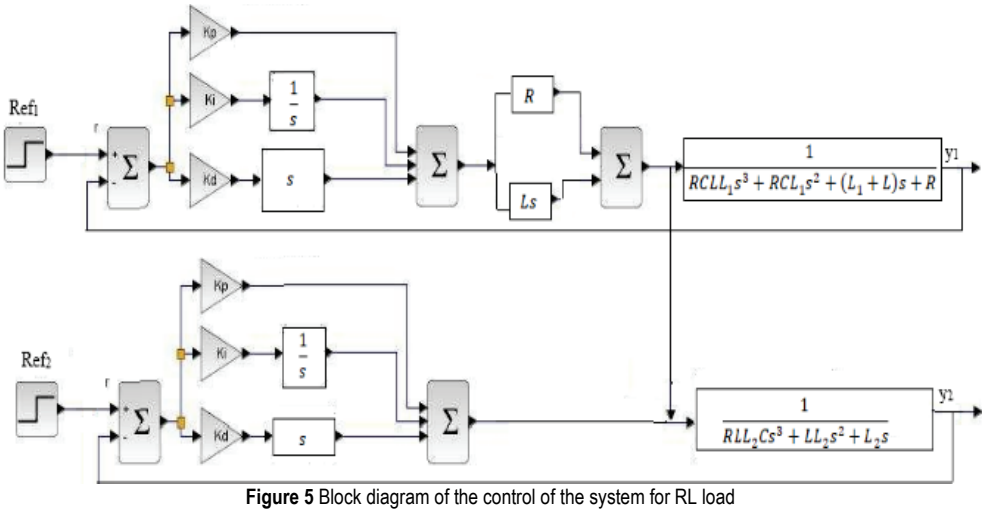

Figure 5 Block diagram of the control of the system for RL load

$$\begin{bmatrix}F_{\mathrm{S1}}\\F_{\mathrm{S2}}\end{bmatrix} = \begin{bmatrix}\frac{R+Ls}{RCLL_1s^3+RCL_1s^2+(L_1+L)s+R} & 0\\ 0 & \frac{R+Ls}{RCLL_2Cs^3+LL_2s^2+L_2s}\end{bmatrix}\begin{bmatrix}\frac{t_1}{(t_1+t_2)}\\ \frac{t_2}{(t_1+t_2)}\end{bmatrix} \tag{29}$$

$$\begin{bmatrix}F_{\mathrm{S1}}\\F_{\mathrm{S2}}\end{bmatrix} = \begin{bmatrix}\frac{(L+K_{\mathrm{d}})s^2+(K_{\mathrm{p}}+R)s+K_{\mathrm{i}}}{RCLL_1s^4+RCL_1s^3+(L_1+L_2+K_{\mathrm{d}})s^2+(R+K_{\mathrm{p}})s+K_{\mathrm{i}}} & 0\\ 0 & \frac{(L+K_{\mathrm{d}})s^2+(K_{\mathrm{p}}+R)s+K_{\mathrm{i}}}{RCLL_2s^4+LL_1s^3+(L_2+K_{\mathrm{d}})s^2+(K_{\mathrm{p}})s+K_{\mathrm{i}}}\end{bmatrix}\begin{bmatrix}\frac{t_1}{(t_1+t_2)}\\ \frac{t_2}{(t_1+t_2)}\end{bmatrix} \tag{30}$$

When the total t time is considered as the working time of the two modes, the working rates to be determined by the time durations of the two functions are as given in the matrix as in Eq. (29). PID can be applied to the mathematical model

of the generated power circuit for R load as shown in the equation matrix as in Eq. (30). The block diagram of the application of the controller to the system at the RL load is as given in Fig. 5.

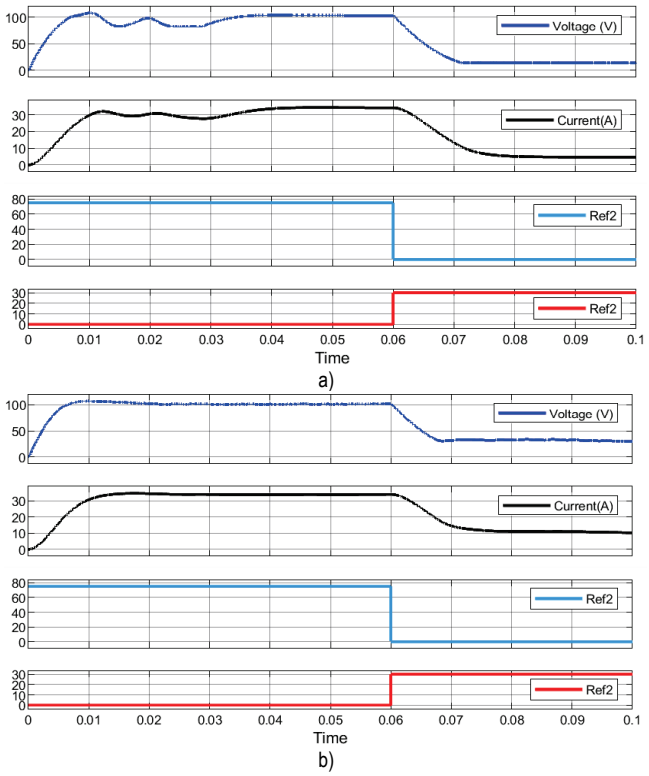

Figure 6 a) PI control for RL load, b) PID control for RL load

For the RL load, the mathematical models of the transfer functions are created in the application of the circuit, where R = 3 ohm and L = 10 mH. When the system is controlled with P = 5 and I = 1 values and PI controls, the current and voltage on the load are formed as given in Fig. 6a. The settling time of current and voltage takes place in 0.038 s. For Boost mode, while 102 V voltage is applied to the load, the current passing through the load is 33.9 A. The electrical energy power conversion obtained for RL load in boost mode is 3457.8 W. For Buck mode, while a voltage of 33 V can be applied to the load on the load, a current of 11 A flows over the load. The electrical energy power conversion obtained for RL load in buck mode is 363 W. When the system is controlled by PID controls with P = 5, I = 1 and D = 0.2 values, the current and voltage on the load are formed as given in Fig. 6b. The settling time of current and voltage takes place in 0.01 s. This provides a 73.6% improvement in the settling time. For Boost mode, while 101 V voltage is applied to the load, the current passing through the load is 33.6 A. For Buck mode, while a voltage of 33 V can be applied to on the load, a current of 11 A passes through the load.

In Fig. 7, the PID Controlling signal outputs of the RLC and the PWMs controlled by the Controllers are given. The first PID controller, which controls the boost mode for up to 0.6 s, after the active control signals on the system for 0.6 s, the Second PID control for Buck mode at load of RL is activated and controls the system. Fig. 8 shows the controller output signals and controlled PWMs while the PI for RL of load is controlling the system. The first PI controller, which controls the boost mode up to 0.6 s for RL load, the Second PI is runnig for the Buck mode and controls the system for RL load. Since PI Control is not sufficient for the boost mode, the PWMs cannot control enough to give the desired output and It is observed that the PWM is given to the system equally and linearly. It is observed that the linearity of the PWMs changes in cases where the controller is made effective, but the linearity of the PWMs does not deteriorate in cases where effective control is not provided.

The circuit model of the converter circuit for R, L and C load is given in Fig. 9. The mathematical models of the transfer function of the circuit according to the series connected RLC load can be arranged as follows.

$$V_{dc} = V_i = L_{L1}\left[L_1 s + \left(\frac{1}{R + Ls + \frac{1}{Cs}} + Cs\right)^{-1}\right] \tag{31}$$

$$V_{dc} = V_i = L_{L1}\left[L_1 s + \left(\frac{1}{\frac{RCs + CsLs + 1}{Cs}} + Cs\right)^{-1}\right] \tag{32}$$

$$V_i = L_{L1}\left[L_1 s + \left(\frac{Cs}{RCs + CsLs + 1} + Cs\right)^{-1}\right] \tag{33}$$

$$V_i = L_{L1}\left[L_1 s + \left(\frac{Cs + CsRCs + CsCsLs + Cs}{RCs + CsLs + 1}\right)^{-1}\right] \tag{34}$$

$$V_i = L_{L1}\left[L_1 s + \left(\frac{RC^2 s^2 + LC^2 s^3 + 2Cs}{RCs + CsLs + 1}\right)^{-1}\right] \tag{35}$$

$$V_i = L_{L1}\left[L_1 s + \left(\frac{RCs + CLs^2 + 1}{RC^2 s^2 + LC^2 s^3 + 2Cs}\right)\right] \tag{36}$$

$$V_i = L_{L1}\left(\frac{C^2 LL_1 s^4 + L_1 RC^2 s^3 + 2L_1 Cs^2 + RCs + CLs^2 + 1}{RC^2 s^2 + LC^2 s^3 + 2Cs}\right) \tag{37}$$

$$V_i = L_{L1}\left[\frac{C^2 LL_1 s^4 + L_1 RC^2 s^3 + (2L_1 C + CL)s^2 + RCs + 1}{RC^2 s^2 + LC^2 s^3 + 2Cs}\right] \tag{38}$$

$$F_{S1} = \frac{I_{L1}\left(\frac{RCs + CLs^2 + 1}{RC^2 s^2 + C^2 Ls^3 + 2Cs}\right)}{I_{L1}\left(\frac{C^2 LL_1 s^4 + L_1 RC^2 s^3 + (2L_1 C + CL)s^2 + RCs + 1}{RC^2 s^2 + C^2 Ls^3 + 2Cs}\right)} \tag{39}$$

$$F_{S1} = \left(\frac{RCs + CLs^2 + 1}{RC^2 s^2 + C^2 Ls^3 + 2Cs}\right)\left(\frac{RC^2 s^2 + C^2 Ls^3 + 2Cs}{C^2 LL_1 s^4 + L_1 RC^2 s^3 + (2L_1 C + CL)s^2 + RCs + 1}\right) \tag{40}$$

$$F_{S1} = \left[\frac{CLs^2 + RCs + 1}{C^2 LL_1 s^4 + RC^2 L_1 s^3 + (2L_1 C + CL)s^2 + RCs + 1}\right] \tag{41}$$

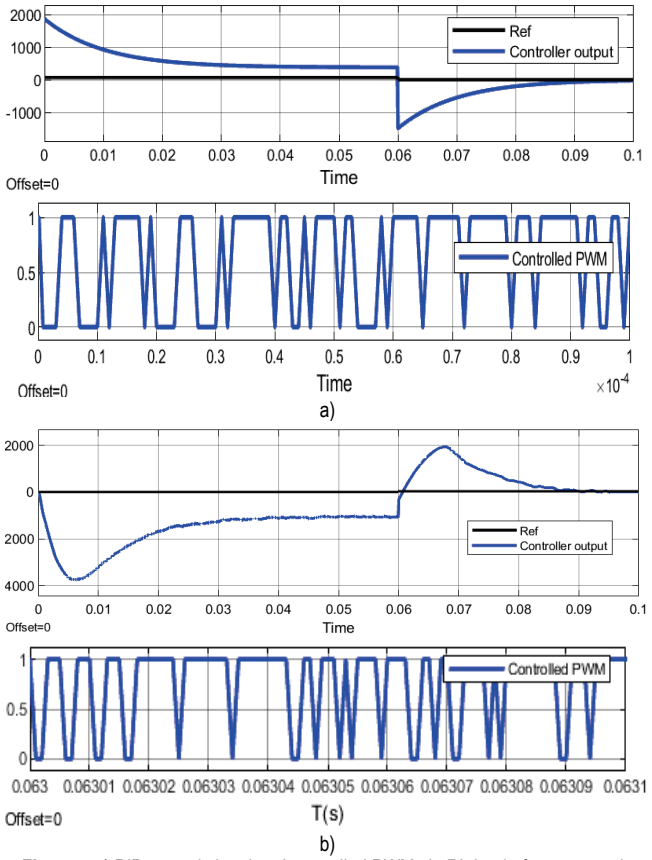

Figure 7 a) PID control signal and controlled PWMs in RL load of my system in boost mode, b) a) PID control signal and controlled PWMs in RL load of my system in buck mode

For F_{S2}, system transfer function calculated as below:

$$V_{dc} = V_i = I_{L2} L_2 s \tag{42}$$

$$V_o = I_{L2}\left(\frac{CLs^2 + RCs + 1}{RC^2 s^2 + C^2 Ls^3 + 2Cs}\right) \tag{43}$$

$$F_{S2} = \frac{V_o}{V_i} = \frac{I_{L2}\left(\frac{CLs^2 + RCs + 1}{RC^2 s^2 + C^2 Ls^3 + 2Cs}\right)}{I_{L2} L_2 s} \tag{44}$$

$$F_{S2} = \left(\frac{CLs^2 + RCs + 1}{C^2 L_2 Ls^4 + RC^2 L_2 s^3 + 2L_2 Cs^2}\right) \tag{45}$$

When the total t time is considered as the working time of the two modes, the working rates to be determined by the time durations of the two functions are as given in the matrix form below.

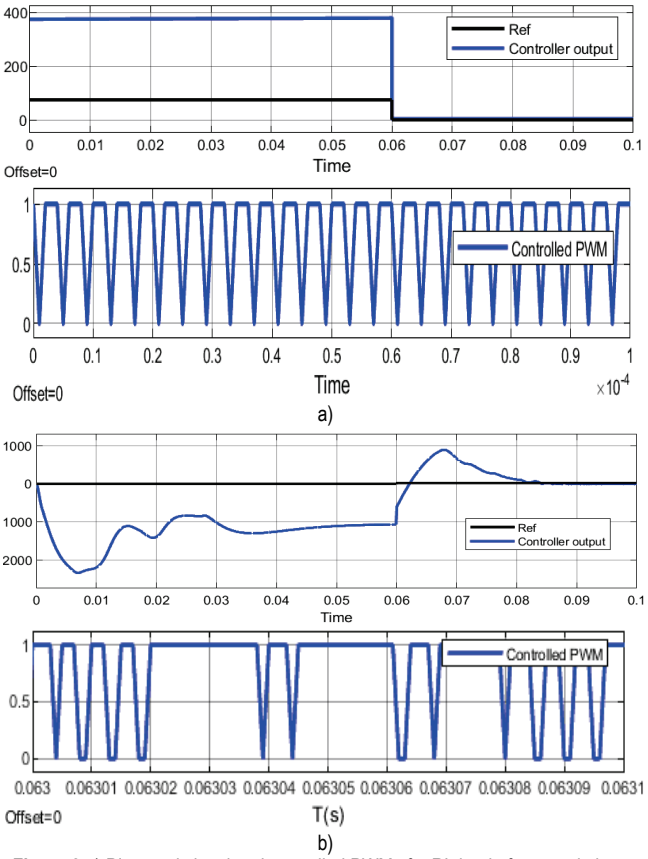

Figure 8 a) PI control signal and controlled PWMs for RL load of system in boost mode, b) a) PI control signal and controlled PWMs in RL load of system in buck mode

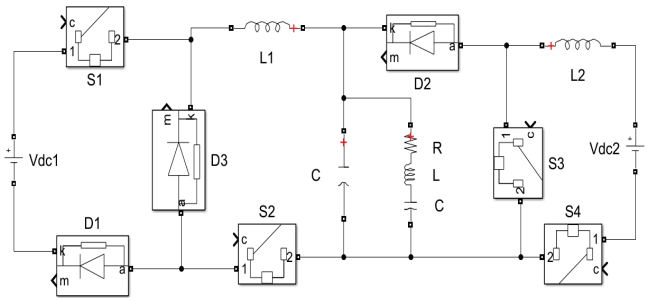

Figure 9 Power circuit for RLC load

$$\begin{bmatrix} F_{S1} \\ F_{S2} \end{bmatrix} = \begin{bmatrix} \dfrac{CLs^2 + RCs + 1}{C^2 LL_1 s^4 + RC^2 L_1 s^3 + (2CL_1 + CL)s^2 + RCs + 1} & 0 \\ 0 & \dfrac{CLs^2 + RCs + 1}{C^2 LL_2 s^4 + RC^2 L_2 s^3 + 2CL_2 s^2} \end{bmatrix} \begin{bmatrix} \dfrac{t_1}{(t_1 + t_2)} \\ \dfrac{t_2}{(t_1 + t_2)} \end{bmatrix} \tag{46}$$

Fig. 10 gives the control block diagram of the system at the RLC load. For the RLC load, the mathematical models of the transfer functions are created in the application of the circuit, where R = 3 ohm, C = 50 mF and L = 10 mH. When the system is controlled with P = 5 and I = 1 values and PI controls, the current and voltage on the load are formed as given in Fig. 11a. The settling time of current and voltage takes place in 0.038 s. For Boost mode, while 106 V voltage

is applied to the load, the current passing through the load is 30 A. For Buck mode, while a voltage of 37 V can be applied to the load on the load, a current of 10A flows over the load. When the system is controlled by PID controls with $P = 5$, $I = 1$ and $D = 0.2$ values, the current and voltage on the load are formed as given in Fig. 11b. The settling time of current and voltage takes place in 0.02 s. This provides a 47.6% improvement in the settling time. For Boost mode, while 106 V voltage is applied to the load, the current passing through the load is 30 A. For Buck mode, while a voltage of 30 V can be applied to on the load, a current of 10 A passes through the load.

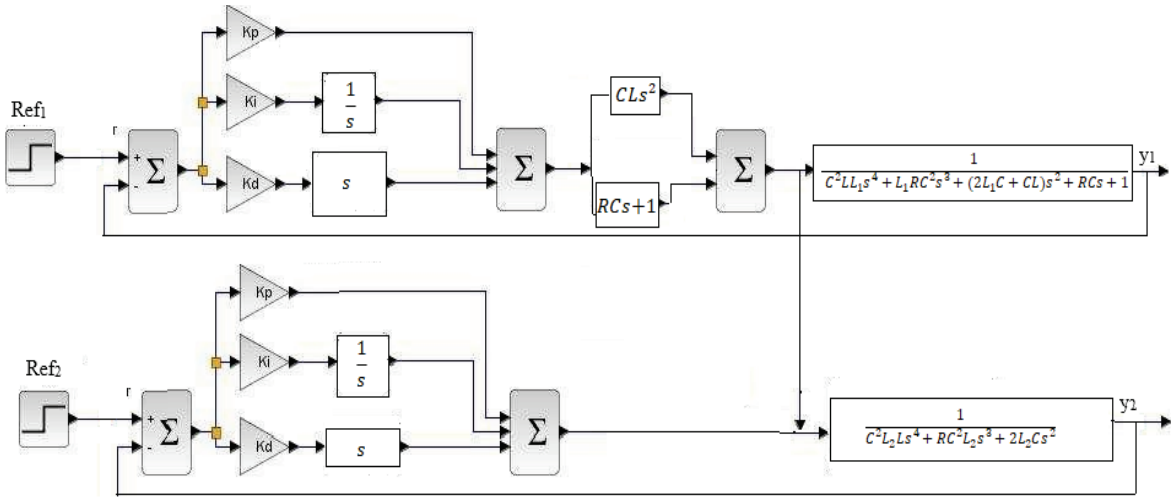

Figure 10 The control block diagram of the system at the RLC load

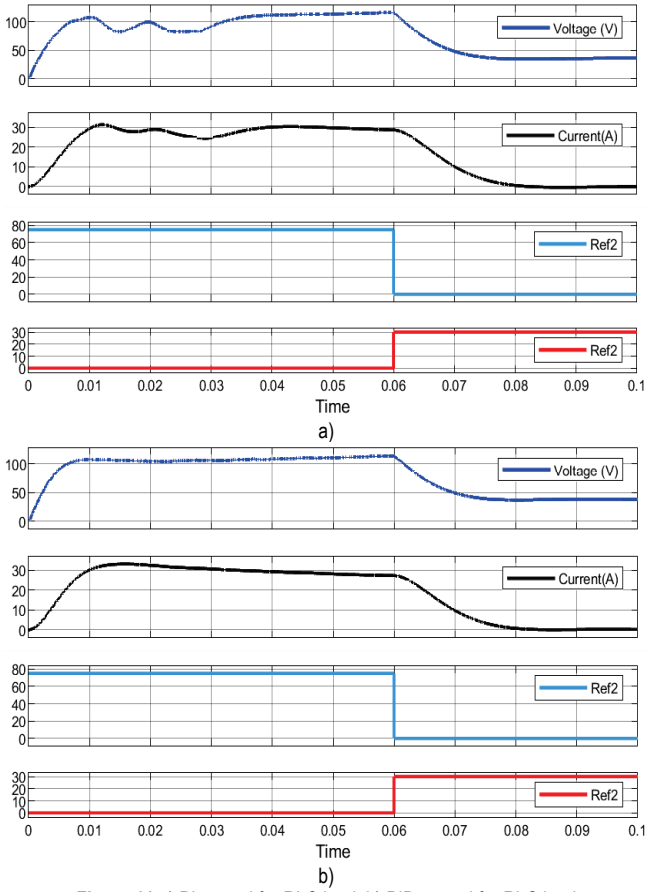

Figure 11 a) PI control for RLC load, b) PID control for RLC load

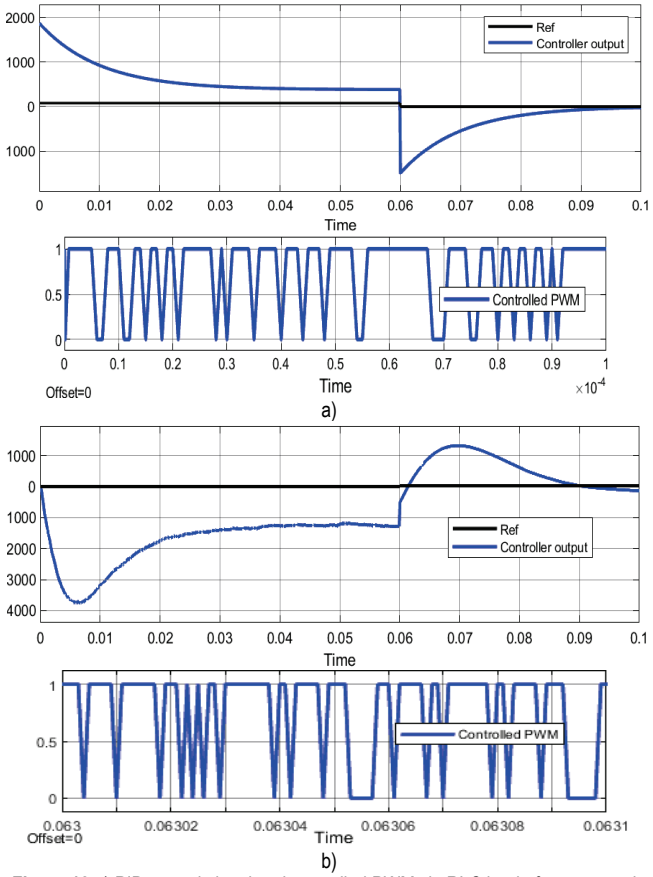

Figure 12 a) PID control signal and controlled PWMs in RLC load of my system in boost mode, b) PID control signal and controlled PWMs in RLC load of system in buck mode

In Fig. 12, the PID Control signal outputs at the RLC load connected in the system and the PWMs controlled are

given. The first PID controls the boost mode for up to 0.6 s in the first reference value, after the control signals are operated on the system for 0.6 s, the Second PID for buck mode is operated and controls the system for RLC load in the other reference.

Fig. 13 shows the controller output signals and controlled PWMs when the PI controller for RLC load controls the system. The first PID controller is operating the boost mode up to 0.6 s at RLC load. After the active control signals are on the system for 0.6 s at the first part reference value, the Second PID control is activated for the buck mode and controls the system at the second part reference value. In obtained the results, the PWMs cannot control enough to give the desired output since PI Control is not sufficient for the boost mode and it is observed that the PWM is given to the system equally and linearly.

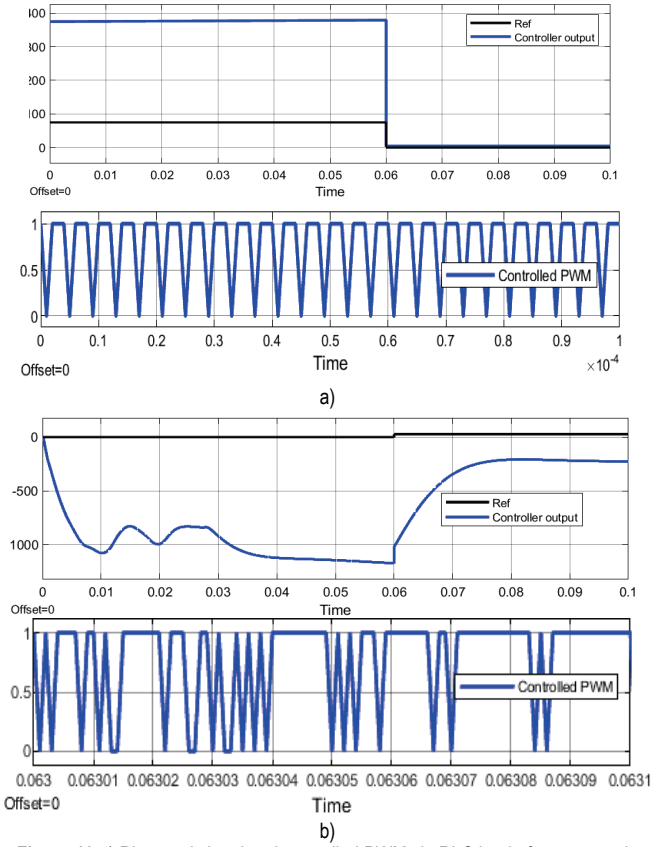

Figure 13 a) PI control signal and controlled PWMs in RLC load of my system in boost mode, b) PI control signal and controlled PWMs in RLC load of system in buck mode

The circuit model for the application formed by parallel loads is given in Fig. 14. One of the parallel connected loads is the series RL load. R values at load are equal. The mathematical models of the transfer function of the circuit according to the series and parallel connected *R* and RL loads can be arranged as follows.

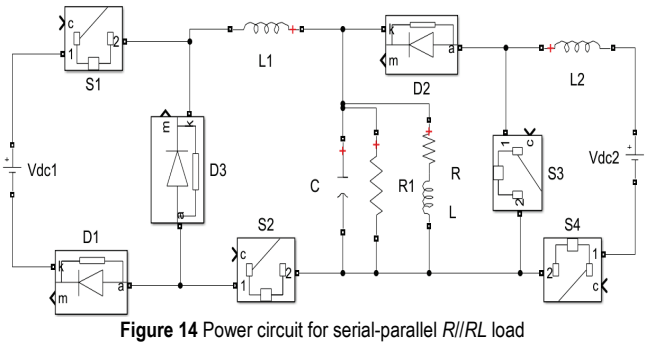

Figure 14 Power circuit for serial-parallel *R*//*RL* load

$$V_{dc} = V_i = L_{L1}\left[L_1 s + \left(\frac{1}{R+Ls} + \frac{1}{R} + Cs\right)^{-1}\right] \quad (47)$$

$$V_i = I_{L1}\left[\frac{CLL_1 s^3 + (L_1R^2C + LL_1)s^2 + (2RL_1 + L)s + R}{LCs^2 + (R^2C + L)s + 2R}\right] \quad (48)$$

$$V_o = I_{L1}\left[\frac{R^2 + Ls}{LCs^2 + (R^2C + L)s + 2R}\right] \quad (49)$$

$$F_{S1} = \frac{I_{L1}\left[\frac{R^2 + Ls}{LCs^2 + (R^2C + L)s + 2R}\right]}{I_{L1}\left[\frac{LL_1Cs^3 + (L_1R^2C + LL_1)s^2 + (2RL_1 + L)s + R^2}{LCs^2 + (R^2C + L)s + 2R}\right]} \quad (50)$$

$$F_{S1} = \left[\frac{R^2 + Ls}{RLL_1Cs^3 + (L_1R^2C + LL_1)s^2 + (2RL_1 + L)s + R^2}\right] \quad (51)$$

For F_{S_2}, system transfer function calculated as below:

$$V_{dc} = V_i = I_{L2}L_2 s \quad (52)$$

$$V_o = I_{L2}\left[\frac{R^2 + Ls}{LCs^2 + (R^2C + L)s + 2R}\right] \quad (53)$$

$$F_{S2} = \frac{V_o}{V_i} = \frac{I_{L2}\left[\frac{R^2 + Ls}{LCs^2 + (R^2C + L)s + 2R}\right]}{I_{L2}L_2 s} \quad (54)$$

$$F_{S2} = \left[\frac{R + Ls}{LL_2Cs^3 + (L_2R^2C + L_2L)s^2 + 2RL_2 s}\right] \quad (55)$$

When the total *t* time is considered as the working time of the two modes, the working rates to be determined by the time durations of the two functions are as given in the matrix form as in Eq. (56). PID can be applied to the mathematical model of the generated power circuit for *R* load as shown in matrix form as in Eq. (57).

$$\begin{bmatrix} F_{S1} \\ F_{S2} \end{bmatrix} = \begin{bmatrix} \frac{R^2 + Ls}{RLL_1Cs^3 + (L_1R^2C + LL_1)s^2 + (2RL_1 + L)s + R^2} & 0 \\ 0 & \frac{R + Ls}{LL_2Cs^3 + (L_2R^2C + L_2L)s^2 + 2RL_2 s} \end{bmatrix} \begin{bmatrix} \frac{t_1}{(t_1 + t_2)} \\ \frac{t_2}{(t_1 + t_2)} \end{bmatrix} \quad (56)$$

$$\begin{bmatrix} F_{S1} \\ F_{S2} \end{bmatrix} = \begin{bmatrix} \dfrac{(L+K_d)s^2+(K_p+R^2)s+K_i}{RLL_1Cs^4+(L_1R^2C+LL_1)s^3+(2RL_1+L+K_d)s^2+(R^2+K_p)s+K_i} & 0 \\ 0 & \dfrac{(L+K_d)s^2+(K_p+R^2)s+K_i}{RLL_2Cs^4+(L_2R^2C+LL_2)s^3+(2RL_2+K_d)s^2+(K_p)s+K_i} \end{bmatrix} \begin{bmatrix} \dfrac{t_1}{(t_1+t_2)} \\ \dfrac{t_2}{(t_1+t_2)} \end{bmatrix} \quad (57)$$

After the transfer function equations created for serial parallel RL load, 3-ohm values for R load values and 10 mH values for L load values are selected. When the system is controlled with P = 5 and I = 1 values and PI controls, the current and voltage on the load are formed as given in Fig. 15a. The settling time of current and voltage takes place in 0.028 s. For Boost mode, while 74 V voltage can be applied to the load, the current passing through the load is 49.5 A. For Buck mode, while a voltage of 32 V can be applied to the load on the load, a current of 20 A flows over the load. When the system is controlled by PID with P = 5, I = 1 and D = 0.2 values, the current and voltage on the load are formed as given in Fig. 15b. The settling time of current and voltage takes place in 0.01 s. This provides a 64.28% improvement in the settling time. For Boost mode, while 74 V voltage is applied to the load, the current passing through the load is 20 A. For Buck mode, while a voltage of 30 V can be applied to on the load, a current of 10 A passes through the load. PI and PID controller performance results of DC-DC converses with complex load structures are given in the Tab. 1.

Table 1 PI and PID controller performance results of DC-DC converses with complex load structures

	R-load				RL-Load			
	Current	Voltage	Power	Settling time	Current	Power	Voltage	Settling time
PI	33.6 A	101 V	3393.6 W	0.04 s	33.9 A	3457.8 W	102 V	0.038 s
PID	33.6 A	101 V	3393.6 W	0.01 s	33.9 A	3457.8 W	102 V	0.016 s
	RLC Load				Seri-Parallel R/RL Load			
	Current	Voltage	Power	Settling time	Current	Power	voltage	Settling time
PI	30 A	106 V	3180 W	0.38 s	49.5 A	3663 W	74 V	0.3 s
PID	30 A	106 V	3180 W	0.2 s	49.5 A	3663 W	74 V	0.1 s

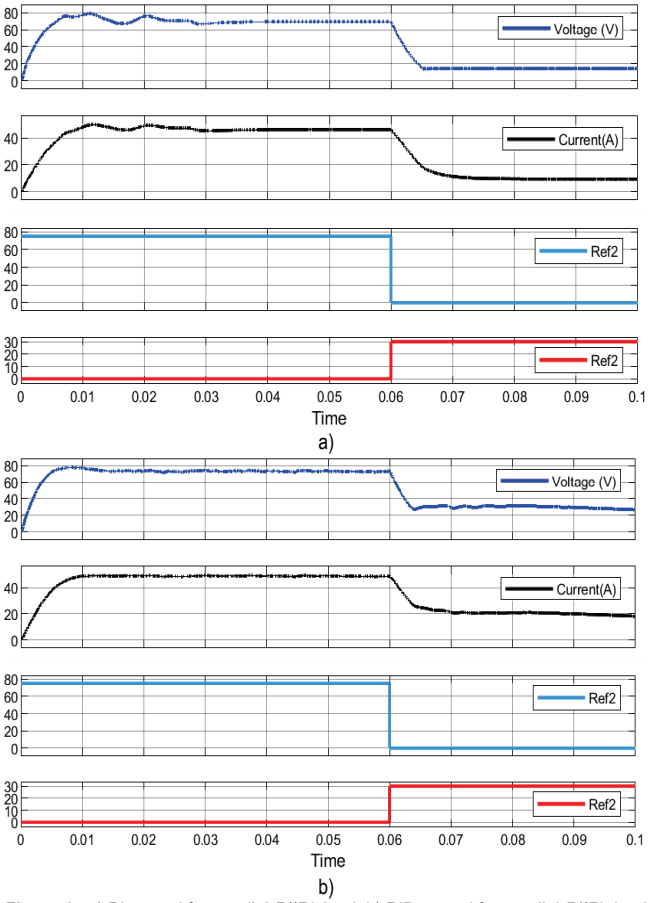

Figure 15 a) PI control for parallel *R*//*RL* load, b) PID control for parallel *R*//*RL* load

3 CONCLUSIONS

This article gives mathematical applications of transfer functions of complex loaded DC-DC converter and PID control of this complex loaded power system. This converter provides two-way operation of the system by using two different fixed input references through power switches added to the converter's general structures. In the first application of the proposed system with R load, PI control provides the settling time of the load current and voltage of the system in 0.04 s, while PID control provides the settling time as 0.01 s. In the applications to be made for RL and RLC, mathematical models of the circuit are derived for these complex load cases. In applications made for RL load, PI control ensures that the load current and voltage are settled at 0.038 s, while PID control provides 0.01 s of the settling time. In the studies, while the mathematical analysis of power circuits with complex load states is made, system improvement is achieved.

Declaration of Competing Interest

The authors declare that they have no known competing financial interests or personal relationships that could have appeared to influence the work reported in this paper.

Acknowledgments

This research did not receive any specific grant from funding agencies in the public, commercial, or not-for-profit sectors.

4 REFERENCES

[1] Akhtar, M. F., Raihan, S. R. S., Rahim, N. A., Akhtar, M. N., & Abu Bakar, E. (2023). Recent Developments in DC-DC Converter Topologies for Light Electric Vehicle Charging: A Critical Review. *Applied Sciences, 13*, 1676. https://doi.org/10.3390/app13031676

[2] Liu, X. & Wu, X. (2023). A two-stage bidirectional DC-DC converter system and its control strategy. *Energy, 266*, 126462. https://doi.org/10.1016/j.energy.2022.126462

[3] Prodic, A. & Maksimovic, D. (2002). Design of a digital PID regulator based on look-up tables for control of high-frequency DC-DC converters. In *2002 IEEE Workshop on Computers in Power Electronics,*18-22. https://doi.org/10.1109/CIPE.2002.1196709

[4] Buccella, C., Cecati, C., & Latafat, H. (2012). Digital control of power converters—A survey. *IEEE Transactions on Industrial Informatics*, *8*, 437-447. https://doi.org/10.1109/TII.2012.2192280

[6] Can, E. (2022). A new multi-level inverter with reverse connected dual dc to dc converter at simulation. *International Journal of Modelling and Simulation*, *42*, 34-46. https://doi.org/10.1080/02286203.2020.1824451

[7] Can, E. & Sayan, H. H. (2017). The performance of the DC motor by the PID controlling PWM DC-DC boost converter. *Tehnički glasnik*, *11*(4), 182-187.

[8] Can, E. (2022). The inverter with reverse connected double converter driving unbalanced loads. *International Journal of Modelling and Simulation*, *42*(2), 217-226. https://doi.org/10.1080/02286203.2021.1871720

[9] Nallusamy, S. & Rukmani, D. K. (2023). Design and simulation of Arduino Nano controlled DC-DC converters for low and medium power applications. *International Journal of Electrical and Computer Engineering*, *13*(2), 1400-1409. https://doi.org/10.11591/ijece.v13i2.pp1400-1409

[10] Paul, A. & Subramanian, K. (2019). PV-based off-board electric vehicle battery charger using BIDC. *Turkish Journal of Electrical Engineering and Computer Sciences*, *27*, 2850-2865. https://doi.org/10.3906/elk-1804-227

[11] Gueye, D. et al. (2018). Design Methodology of Novel PID for Efficient Integration of PV Power to Electrical Distributed Network. *Int. J. Smart Grid, 2*, 21-32 https://doi.org/10.20508/ijsmartgrid.v2i1.14.g11

[12] Wang, W. Q., Li, M. J., Guo, J. Q., & Tao, W. Q. (2023). A feedforward-feedback control strategy based on artificial neural network for solar receivers. *Applied Thermal Engineering*, 120069. https://doi.org/10.1016/j.applthermaleng. 2023.120069

[13] Bairabathina, S. & Subramani, B. (2023). Design prototype validation, and reliability analysis of a multi-input DC/DC converter for grid-independent hybrid electric vehicles. *International Journal of Circuit Theory and Applications*, 1-31. https://doi.org/10.1002/cta.3533

[14] Punnya Priya, F., Latha, K., & Ramya, K. (2023). Improved Dynamic Performance of the Fuel Cell-Fed Boost Converter Using Super Twisting Sliding Mode Control Strategy. *IETE Journal of Research*, 1-11. https://doi.org/10.1080/03772063.2023.2169776

[15] Ziemba, R. (1988). Use of a programmable logic controller (PLC) for temperature, position, velocity and pressure control of injection molding machinery. In *Conference Record of the 1988 IEEE Industry Applications Society Annual Meeting*, 1397-1404. https://doi.org/10.1109/IAS.1988.25241

[14] Nie, Z. Y., Li, Z., Wang, Q. G., Gao, Z., & Luo, J. (2022). A unifying Ziegler–Nichols tuning method based on active disturbance rejection. *International Journal of Robust and Nonlinear Control*, *32*, 9525-9541. https://doi.org/10.1002/rnc.5848

[16] Can, E. (2023). A Common Capacitor Hybrid Buck-Boost Converter. *Jordan Journal of Electrical Engineering, 9*, 71-83. https://doi.org/10.5455/jjee.204-1666615450

[17] Patel, V. V. (2020). Ziegler-Nichols Tuning Method: Understanding the PID Controller. *Resonance*, *25*, 1385-1397. https://doi.org/10.1007/s12045-020-1058-z

Authors' contacts:

Erol Can
(Corresponding author)
Department of Aviation Electric- Electronics,
School of Civil Aviation,
Erzincan Binali Yıldırım University,
Erzincan, Turkey
cn_e@hotmail.com

Murat Gülnahar
Department of Electrics and Energy,
Vocational School,
Erzincan Binali Yıldırım University,
Erzincan, Turkey